Immobilized sonic hedgehog N-terminal signaling domain enhances differentiation of bone marrow-derived mesenchymal stem cells

James E. Ho,[1,2,3] Eugene H. Chung,[1,3] Samuel Wall,[1,3] David V. Schaffer,[3,4] Kevin E. Healy[1,2,3]
[1]*Department of Bioengineering, University of California at Berkeley, Berkeley, California 94720-1762*
[2]*Department of Materials Science and Engineering, University of California at Berkeley, 370 Hearst Memorial Mining Building, Berkeley, California 94720-1760*
[3]*UCSF/UCB Joint Graduate Group in Bioengineering, University of California, Berkeley, California*
[4]*Department of Chemical Engineering and the Helen Wills Neuroscience Institute, University of California at Berkeley, 201 Gilman Hall, Berkeley, California 94720-1462*

Received 31 August 2006; revised 1 February 2007; accepted 23 February 2007
Published online 28 June 2007 in Wiley InterScience (www.interscience.wiley.com). DOI: 10.1002/jbm.a.31355

Abstract: The signaling domain of Sonic hedgehog (Shh), a potent upstream regulator of cell fate that has been implicated in osteoblast differentiation from undifferentiated mesenchymal cells in its endogenous form, was investigated in an immobilized form as a means for accelerating differentiation of uncommitted cells to the osteoblast phenotype. A recombinant cysteine-modified N-terminal Shh (mShh) was synthesized, purified, and immobilized onto interpenetrating polymer network (IPN) surfaces also grafted with a bone sialoprotein-derived peptide containing the Arg-Gly-Asp (RGD) sequence (bsp-RGD (15)), at calculated densities of 2.42 and 10 pmol/cm^2, respectively. The mitogenic effect of mShh was dependent on the mode of presentation, as surfaces with immobilized mShh and bsp-RGD (15) had no effect on the growth rate of rat bone marrow-derived mesenchymal stem cells (BMSCs), while soluble mShh enhanced cell growth compared to similar surface without mShh supplementation. In conjunction with media supplemented with bone morphogenetic protein-2 and -4, mShh and bsp-RGD (15)-grafted IPN surfaces enhanced the alkaline phosphatase activity of BMSCs compared with tissue culture polystyrene and bsp-RGD (15)-grafted IPN surfaces supplemented with soluble mShh, indicating enhanced osteoblast differentiation. The adhesive peptide bsp-RGD (15) was necessary for cell attachment and proliferation, as well as differentiation in response to immobilized mShh. The addition of immobilized Shh substantially improved the differentiation of uncommitted BMSCs to the osteoblast lineage, and therefore warrants further testing *in vivo* to examine the effect of the stated biomimetic system on peri-implant bone formation and implant fixation. © 2007 Wiley Periodicals, Inc. J Biomed Mater Res 83A: 1200–1208, 2007

Key words: sonic hedgehog; bone marrow-derived mesenchymal stem cells; biomimetic; biointerface

INTRODUCTION

The paradigm of biomimetic surface engineering (BSE) stipulates that monolayer biological coatings, inspired from natural sources, are sufficient to direct specific cell-material interactions and control wound healing in the peri-implant region. Early implementations of BSE focused on surface modification with immobilized peptides,[1–3] where maintenance of stable phenotypes, including osteoblasts, chondrocytes, and neurites was observed *in vitro*.[3–7] However, translation of these *in vitro* efforts into the clinical domain have largely failed, where *in vivo* studies investigating RGD-peptide modified implants provide only weakly statistically significant evidence to support the concept that peptide-modified interfaces have a positive effect on bone regeneration in the peri-implant region.[8–12] For example, a 15-amino acid sequence derived from bone sialoprotein that contains the adhesion and mitogenic ligand RGD (bsp-RGD (15)) has been presented to cells using an intrinsically nonfouling interpenetrating polymer network (IPN).[12,13] In spite of impressive *in vitro* studies demonstrating the effectiveness of bsp-RGD (15) in fostering osteoblast differentiation,[14,15] this

Correspondence to: K.E. Healy, University of California at Berkeley, Department of Materials Science and Engineering, 370 Hearst Memorial Mining Building, no. 1760, Berkeley, CA 94720-1760, USA; e-mail: kehealy@berkeley.edu

Contract grant sponsor: National Institutes of Health; contract grant number: AR43187

peptide was not sufficient to enhance peri-implant bone formation in a rat femoral ablation implant model.[12] Similarly, studies by Elmengaard et al.,[9] who examined both loaded and unloaded RGD-coated titanium implants placed in the distal femur and proximal tibiae of canines, respectively, did not show a statistically significant difference in push-out strength between the implants treated with a RGD peptide coating compared with controls. These data suggest that a RGD-containing peptide grafted to an implant surface is neither sufficient for accelerating the rate of bone formation in the peri-implant region nor for enhancing the interfacial shear strength between the implant and bone.

In light of these findings, a change in design of the biomimetic surface was proposed, as improvement in peri-implant bone formation and interfacial bonding may require use of more potent molecules, such as growth factors and morphogenetic proteins. Precedence for growth factor immobilization comes from observations with epidermal growth factor (EGF), which retained its biological activity when tethered to a surface via poly(ethylene glycol) (pEG), but not when physically adsorbed.[16] We chose to investigate Sonic hedgehog (Shh) as an alternative to the oft studied bone morphogenetic proteins (BMPs) and transforming growth factor-β that stimulate bone remodeling in the peri-implant region.[17]

Shh is a potent signaling protein that regulates proliferation, differentiation, and cellular patterning across a wide range of cell types. Shh signals cells through the two transmembrane proteins, Patched (Ptc), which is the direct binding target of Shh and Smoothened (Smo), a protein with homology to G-protein-coupled receptors whose activity is inhibited by the unbound form of Ptc.[18] Together, these proteins regulate the transcriptional levels of the Ptc gene itself as well as the Gli family of transcriptional effectors that govern the cellular response.[18] Shh has strong osteogenic potential, and the developmental relationship between the family of hedgehog proteins and BMPs has been established.[19–24] This association is also apparent from *in vitro* tissue culture and recent *in vivo* studies,[25] which suggest a synergistic cooperation between BMPs and Shh in the promotion of osteoblast differentiation from progenitor cells. Shh also retains its activity in surgically-treated defects where these cells are present, as Shh-expressing cells implanted into a rabbit cranial defect model within an alginate/collagen matrix statistically improved bone regeneration compared with matrices loaded with cells not expressing Shh.[26] These observations support the selection of Shh as a novel molecule to promote bone regeneration in the peri-implant region, where BMP-2, BMP-4, and BMP-7 are upregulated during the wound healing process.[27,28]

In this study, we examined whether tethered Shh could yield the same osteogenic effect as soluble Shh, and if immobilization affected the differentiating and mitogenic effect of Shh. Since the activation of Smo via Shh does not seem to require internalization of Shh, we propose that grafting of Shh to a surface should not attenuate its activity.

The first component of the study was dedicated towards developing a ligand density characterization assay, modeled after a cleavable fluorescent protocol designed to quantitatively detect bound bsp-RGD (15).[29] Subsequently, a cell culture model reflective of the cellular complexity found in the bone marrow environment was implemented to assess the mitogenic and differentiating effects of conjugated mShh. Adult bone marrow-derived mesenchymal stem cells (BMSCs) were used, as these cells can differentiate into several phenotypes, thus providing a discerning measure of whether differentiation conditions are modulated by the grafted Shh. In addition, the cell population harvested from the bone marrow is heterogeneous in nature and better reflects the cell distribution and level of maturity at the implant interface in the rat femoral ablation model, which we have previously used to assess the effect of biomimetic coatings *in vivo*.[12,30,31] The effect of soluble BMP-2/4 supplemented to the growth media was also investigated, as it was previously observed that bone formation enhancement due to soluble Shh was further enhanced by BMP-2/4-dependent pathways *in vivo*.[32]

MATERIALS AND METHODS

Production of mShh

Established recombinant DNA techniques were used to synthesize a modified form of the complete Shh molecule (mShh).[33] PCR was used to engineer mShh to include a cysteine residue on its C-terminus for covalent attachment to the IPN using previously described bioconjugation methods.[34] In addition, valine and isoleucine residues were introduced to the N-terminus to increase potency by mimicking the hydrophobic palmitic acid modification of endogenous Shh, and a 6× histidine (His) tag was added to the C-terminus for purification via nickel affinity chromatography. These modifications were verified through DNA sequencing of the expression vector, and cloning details are available upon request.

Characterization of mShh-IPN conjugation

The IPN was grafted onto TCPS stripwells as described previously,[35] and the ability to create a specific covalent attachment between the sulfhydryl group of mShh and maleimide-terminated IPN surfaces was verified and char-

TABLE I
Descriptions and Abbreviations of Surfaces and Media Supplementations Used

Base Surface Description	Media Supplementations	Group Abbreviation
TCPS	None	TCPS
	mShh	TCPS S
	BMP-2, BMP-4	TCPS 24
	mShh, BMP-2, BMP-4	TCPS S24
IPN	None	IPN
IPN/RGD	None	IPN/RGD
	mShh	IPN/RGD S
	BMP-2, BMP-4	IPN/RGD 24
	mShh, BMP-2, BMP-4	IPN/RGD S24
IPN/RGD/Shh	None	IPN/RGD/Shh
	BMP-2, BMP-4	IPN/RGD/Shh 24
IPN/Shh	None	IPN/Shh
	BMP-2, BMP-4	IPN/Shh 24

A slash in the group name denotes immobilization.

acterized using a fluorescent microplate assay. The mShh N-terminal signaling domain was left with a 6× His tag towards its C-terminus, which was subsequently used to specifically bind the protein to nickel-activated horseradish peroxidase (HRP) (Pierce, Rockford, IL). Various concentrations of mShh conjugated with HRP were incubated in IPN-covered black microplates (Greiner Bio-One) overnight at 4°C using 0.2*M* carbonate–bicarbonate coating buffer at pH 9.4 (Pierce), supplemented with 100 n*M* tris(2-carboxyethyl) phosphine hydrochloride (TCEP·HCl) to prevent disulfide bond formation. Remaining unreacted maleimide groups were not quenched as the high pH removed the concern of possible reactivity. After rinsing in PBS with 0.15*M* NaCl and 0.5% v/v Nonidet P-40 to remove loosely bound protein, QuantaBlu (Pierce), a fluorogenic probe for HRP, was introduced to yield a soluble product with excitation/emission wavelengths of 325/420 nm. About 100 μL of the 25 n*M* HRP probe working solution was added to each well for 15 min at 25°C. Following several more rinses, 100 μL of the QuantaBlu solution was added for 30 min at 25°C, whereupon the fluorogenic reaction was stopped using a solution provided by the manufacturer. The fluorescent solution (100 μL) was then transferred from the transparent stripwells to a black microplate and read using a SpectraMax Gemini XS fluorimeter (Molecular Devices, Sunnyvale, CA). Molar quantities of mShh grafted to IPN surfaces were converted from HRP probe solution standards based on a dissociation constant, k_D, of 1 μ*M* between the imidazole group and nickel,[36] and a factor of 3 to account for the number of nickel groups per HRP probe. Given an input HRP probe concentration of 25 n*M*, the conversion factor from bound HRP molar density to immobilized mShh molar density was 3.22.

Rat BMSC isolation and expansion

Adult BMSC isolation procedures were approved by the UC Berkeley Animal Care and Use Committee. Sprague-Dawley rats ~6 months of age and weighing 425–450 g were obtained from Harlan (Indianapolis, IN). Rats were sacrificed by anesthetizing in a CO_2 chamber for 5 min followed by cervical dislocation. After the hind legs were denuded of muscle and the femurs extracted from the carcass, the epiphyses of the femur were removed to expose the bone marrow. A 23-gauge needle filled with Dulbecco's modified Eagle's media (DMEM) supplemented with 100 U/mL penicillin/streptomycin, 2.5 μg/mL fungizone, 1 m*M* sodium pyruvate, and 10 m*M* HEPES was used to flush the marrow contents into a sterile 50-mL tube. Tube contents were filtered using a 40-μm nylon cell strainer, centrifuged at 900*g* for 5 min, and resuspended in 10 mL Iscove's modified Eagle's media containing 100 U/mL penicillin/streptomycin, 2.5 μg/mL, fungizone, 1 m*M* sodium pyruvate, and 20% FBS. Cells present within each tube were plated and fed every 2–3 days with fresh DMEM containing 100 U/mL penicillin/streptomycin, 2.5 μg/mL fungizone, 1 m*M* sodium pyruvate, and 15% FBS. After proliferating to ~50% confluence, cells were passaged and the feeding process was repeated to remove nonadherent cells. Cells were used after the second passage (P2).

Experimental groups

IPN surfaces were prepared in three configurations (Table I), using the maleimide-terminated surface to graft biofunctional groups in accordance with previously established procedures[15,35]: (1) bsp-RGD (15) (Cys-Gly-Gly-Asn-Gly-Glu-Pro-Arg-Gly-Asp-Thr-Tyr-Arg-Ala-Tyr-NH_2) (Γ = 10 pmol/cm^2); (2) bsp-RGD (15) and Shh-grafted IPN; and, (3) Shh-grafted IPN. In the second group, bsp-RGD (15) was coupled onto IPNs in concert with mShh at an input concentration of 1 μ*M*, with 100 n*M* TCEP·HCl added. TCPS control and the three experimental IPN-biomolecule configurations were further distinguished by various sets of media conditions. For wells without immobilized mShh, media conditions were supplemented at day 2 with either 50 n*M* soluble mShh, a combination of 150 ng/mL BMP-2 and 150 ng/mL BMP-4 (R&D systems, Minneapolis, MN), both mShh and BMP-2/4, or no supplementation (Table I). For wells with immobilized Shh, media conditions were supplemented with BMP-2/4 or nothing. A control IPN group was included with no media supplementation. Proliferation, viability, and differentiation were then tested on the various surfaces using the BMSC cell population according to the schedule displayed in Table II.

Cell proliferation measurement

Cell proliferation was assessed using alamarBlue fluorescent metabolic activity dye (BioSource, Camarillo, CA).

TABLE II
Schedule of *In Vitro* Assays for Testing the Effect of Immobilized Versus Soluble mShh

	Timepoints
Proliferation assay	Days 1, 3, 5, 7 (n = 8 per group)
Differentiation assay	Days 3 (n = 3), 5, 7 (n = 8)
Viability assay	Day 7 (n = 1)

RFU values were fitted to a Verhulst logistic growth model[37] [Eq. (1)] to extract initial attachment (N_o), carrying capacity (K), and growth rate (r) parameters.

$$N(t) = \frac{K}{1 + \left(\frac{K}{N_o} - 1\right)\exp(-rt)} \quad (1)$$

Cell morphology and viability

After 7 days in culture, cells grown on 24-well plates were assessed for viability using a Live/Dead Viability/Cytotoxicity kit (Invitrogen, Carlsbad, CA). Wells were rinsed twice with 300-μL incomplete Dulbecco's phosphate buffered saline (idPBS), aspirated, and incubated for 30 min at room temperature with 300-μL idPBS containing 2-μ*M* Calcein AM and 1-μ*M* ethidium homodimer-1 (EthD-1). Samples were viewed in epifluorescence mode using a Nikon Eclipse TE300 inverted microscope (Nippon Kogaku K. K., Tokyo, Japan) with a 10× objective, 10× eyepiece, and excitation/emission filters appropriate for visualizing calcein (494/518 nm) and EthD-1 (494/635 nm). Images were collected using a Kodak digital camera. Overlay and post-processing of images was performed using Photoshop 5.0 (Adobe Systems, Mountain View, CA) to generate a composite live/dead micrograph.

Cellular differentiation assay

Osteoblast differentiation was measured using 9H-(1,3-dichloro-9,9-dimethylacridin-2-one-7-yl) phosphate (DDAO-phosphate) (Molecular Probes) and its fluorescent product, dimethylacridone (DDAO), which returns the total amount of alkaline phosphatase (ALP) present in a cell lysate.[13] Total ALP activity was further normalized by total protein content using the Micro BCA protein assay reagent kit (Pierce) in accordance with manufacturer instructions.

Statistics and data analysis

Statistics were performed using JMP 5.0 (SAS Institute, Cary, NC). Proliferation and differentiation data for groups of three or more were assessed at each timepoint separately and analyzed using one-way ANOVA followed by *post hoc* Tukey HSD test to establish group-wise significance at the $\alpha = 0.05$ level. Pair-wise analysis was performed using Student's t test on TCPS and IPN + RGD groups featuring mShh-only supplementation and mShh + BMP-2/4 supplementation.

RESULTS

Characterization of mShh grafting

mShh was conjugated via maleimide groups attached to IPN-grafted surfaces at concentrations ranging from 0 to 1000 n*M* (0–1900 ng/well) ($N = 8$). The RFU values measured from the fluorogenic reaction of conjugated HRP were converted to molar graft density and plotted in Figure 1, with the linear curve ($R^2 = 0.998$) extending over the entire range of the dataset. A control experiment using IPN surfaces preblocked with cysteine·HCl prior to mShh conjugation abolished mShh binding. At 1-μ*M* mShh input concentration, $\Gamma_{mShh} = 2.42 \pm 0.47$ pmol/cm^2 on IPN surfaces.

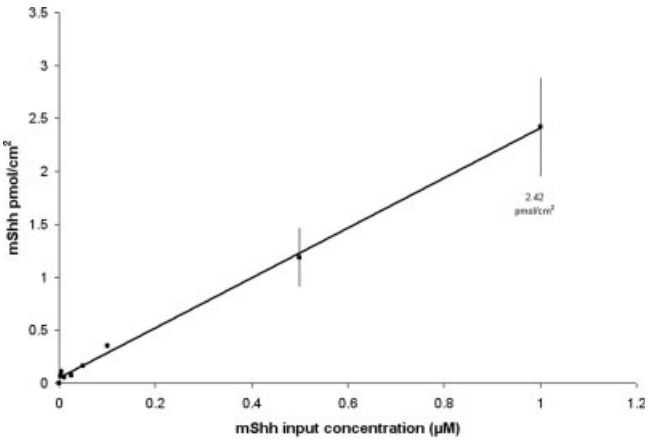

Figure 1. Calibration curve indicating mShh grafting density as a function of input concentration.

In vitro results

Viability

Calcein/EthD-1 fluorescent images of BMSCs after 7 days, under the different conditions outlined in Table I, are displayed in Figure 2. On TCPS surfaces [Fig. 2(A–D)] with various media supplements (none, BMP-2/4, soluble mShh and mShh + BMP-2/4, respectively), cells were well-spread. There were few dead cells and no significant differences between the groups. On IPN/RGD surfaces [Fig. 2(E–H)] with media supplementation identical to images A–D, there were qualitatively a greater number of cells compared with TCPS for the same media condition. Soluble mShh supplementation increased cell number, as IPN/RGD with soluble mShh (IPN/RGD S) had more cells than IPN/RGD with no supplement [Fig. 2(E,G)], and IPN/RGD with soluble mShh + BMP-2/4 (IPN/RGD S24) had more cells than IPN/RGD with BMP-2/4 (IPN/RGD 24) [Fig. 2(F,H)]. A marked increase in cell density was apparent for the IPN/RGD/Shh surface with soluble BMP-2/4 supplementation [Fig. 2(J)]. This increase was dramatic compared to the IPN/RGD surface with soluble mShh in the media [Fig. 2(G)]. Surfaces without the bsp-RGD (15) ligand (i.e., IPN/Shh groups without and with BMP-2/4 supplementation, images K and L, respectively) supported little cell attachment or growth.

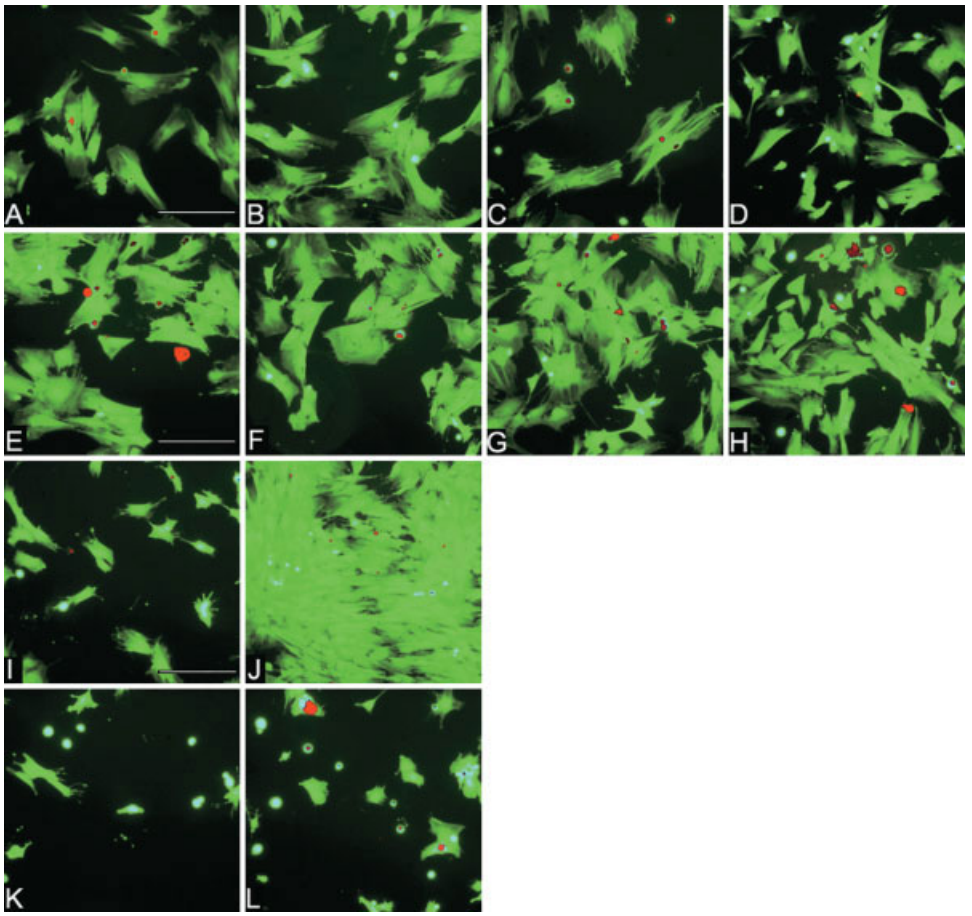

Figure 2. Calcein/EthD-1 fluorescent images of BMSC cells at 7 days in culture, where the base layer description is followed by a code indicating the media supplementation: S = mShh supplementation, 2 = BMP-2 supplementation, 4 = BMP-4 supplementation. A–D: TCPS, TCPS 24, TCPS S, TCPS S24. E–H: IPN/RGD, IPN/RGD 24, IPN/RGD S, IPN/RGD S24. I–J: IPN/RGD/Shh, IPN/RGD/Shh 24. K,L: IPN/Shh, IPN/Shh 24. Scale bar = 200 μm. Group descriptions are detailed in Table I. [Color figure can be viewed in the online issue, which is available at www.interscience.wiley.com.]

Proliferation

The proliferation data on the different surfaces were grouped by media supplementation (Fig. 3). For TCPS groups, only minor differences in alamarBlue RFU values were present at day 1, and by day 7 there were no significant differences in proliferation, despite the addition of various media supplements. The IPN-based groups without bsp-RGD (15) (IPN, IPN/Shh, and IPN/Shh 24) were not able to support cell growth regardless of media supplementation. The IPN/RGD and IPN/RGD/Shh groups supported cell growth and exhibited only minor statistical differences between each other. Without media supplements, the IPN/RGD/Shh surface had fewer cells than TCPS after 7 days. However, when BMP-2/4 was added there were no differences between the surfaces. When soluble mShh was supplied to the IPN/RGD and TCPS surfaces, no differences were observed by days 5 and 7, regardless of further supplementation with BMP-2/4. Logistic curves were fit to the data, and growth rates relative to TCPS are listed in Table III. Full supplementation (i.e., BMP-2/4) provided the highest growth rates, while no supplementation yielded the lowest growth rates. Surfaces containing bsp-RGD (15) had higher growth rates compared with TCPS under similar media conditions, and the surface with the highest growth rate was IPN/RGD/Shh with BMP-2/4 supplementation (Table III).

Differentiation

ALP activity normalized to protein content after 3, 5, and 7 days in culture is displayed in Figure 4. The IPN, IPN/Shh, and IPN/Shh 24 surfaces showed consistently lower ALP activity compared with TCPS. With no supplements, the IPN/RGD surface featured a peak at day 5, while the IPN/RGD/Shh surface showed a continuous rise from day 3 to 7. The IPN/RGD/Shh 24 surface was the highest group at days 3 and 5, with day 5 reaching the highest amount of ALP (27 μU/μg) across all groups and

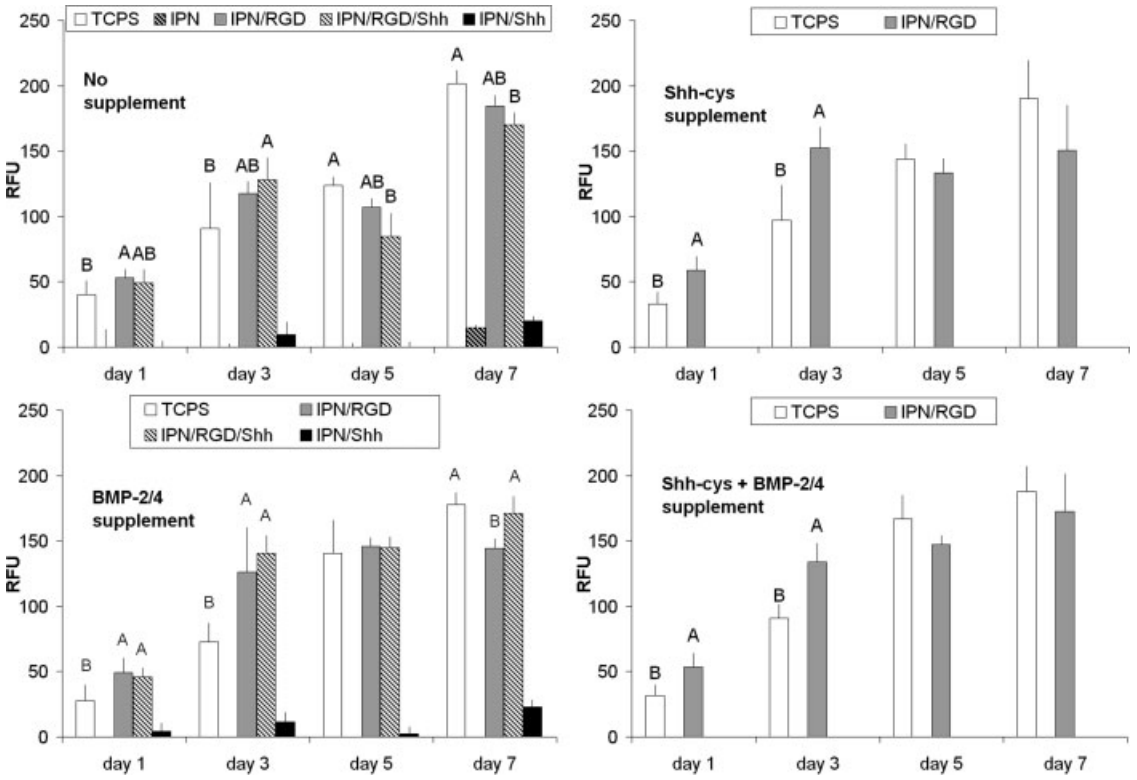

Figure 3. AlamarBlue RFU values for BMSCs, categorized by media supplemention. Groups were statistically compared within each timepoint. Groups not connected by the same letter are significantly different, with A statistically higher than B.

time. Among only the IPN/RGD groups, at days 3 and 5, IPN/RGD S24 surface returned the highest ALP activity. There was no difference in ALP activity between the IPN/RGD S and TCPS S surfaces.

DISCUSSION

We evaluated the effect of immobilized versus soluble mShh in concert with osteogenic factors previously demonstrated to have a synergistic effect with Shh on mesenchymal cell differentiation. A heterogeneous population of primary cells isolated from adult rats, BMSCs, was used to more accurately model the femoral ablation impant model we have previously employed to investigate candidate biomimetic osteogenic surfaces.[31,38] Because our ultimate goal was to develop a system capable of maximally stimulating bone regeneration and implant fixation, two steps were in order. First, we set out to quantify the amount of mShh immobilized. Thereafter, we were able to determine the impact of immobilized mShh on BMSC behavior, among the influence of both adhesion motifs (e.g., bsp-RGD (15)) as well as factors naturally present within the wound bed (e.g., BMP-2 and -4).

Conjugation of mShh to surfaces was successfully performed and characterized. Based on the N-terminal Shh crystal structure[39] (body-centered orthorhombic, $a = 53.7$ Å, $b = 79.0$ Å, $c = 35.4$ Å) and assuming coverage one unit cell thick, maximal mShh

TABLE III
Logistic Growth Rates for BMSCs After 7 days, Relative to TCPS

	r		*r*		*r*
TCPS	1.000	IPN/RGD	1.747	IPN/RGD/Shh	3.472
TCPS S	2.087	IPN/RGD S	4.441	IPN/RGD/Shh 24	4.830
TCPS 2	2.167	IPN/RGD 24	4.420		
TCPS S2	1.472	IPN/RGD S24	3.486		
TCPS 24	2.378				
TCPS S24	2.903			IPN/Shh	N/A
IPN	N/A			IPN/Shh 24	N/A

No fits were possible with IPN and IPN/Shh groups.

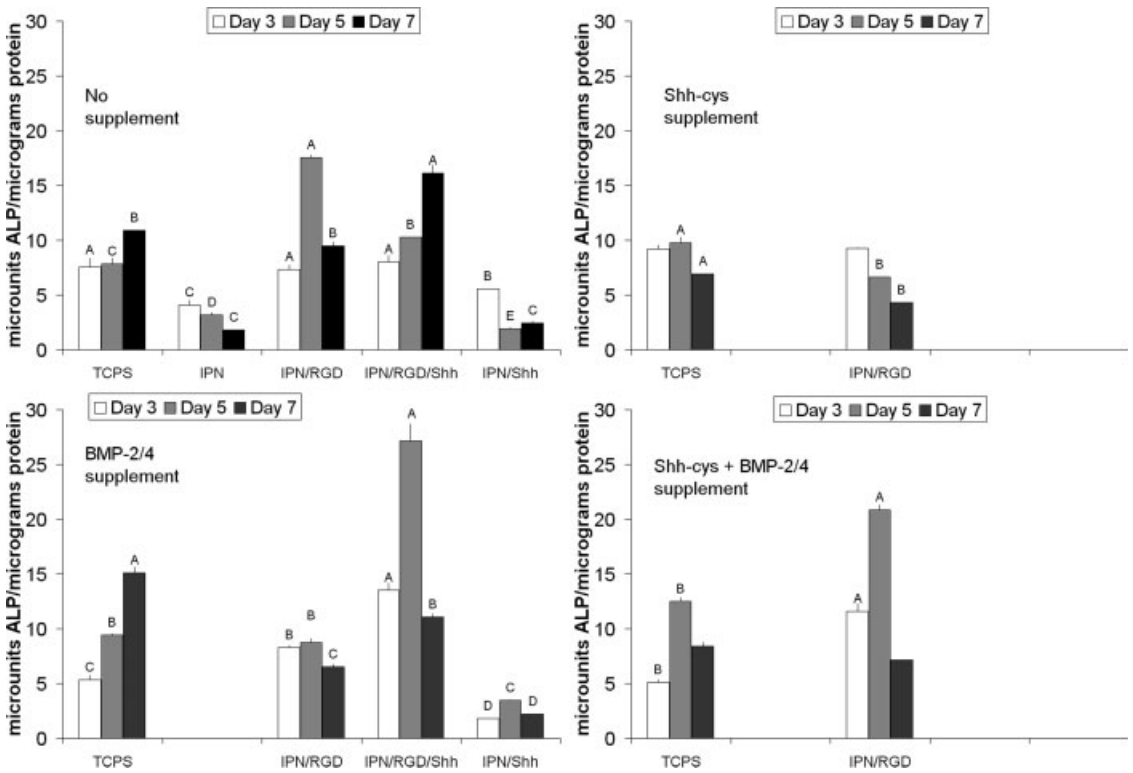

Figure 4. BMSC normalized ALP activity, categorized by media supplementation. Although data was arranged to illustrate timecourse behavior, groups were statistically compared within each timepoint. Groups not connected by the same letter are significantly different, with A statistically higher than B.

monolayer grafting density is theoretically 15.7 pmol/cm^2. At 1 μ*M* mShh input concentration for conjugation to the IPN, the grafting density was estimated to be 2.42 pmol/cm^2, or ~15% of the theoretically calculated maximum monolayer grafting density. A limitation on this estimate was the need for a conversion factor from molar concentration to surface density, which was based on literature values for nickel-imidazole binding.[36] The maximal mShh measured in this study was set due to practical material and cost considerations, although a saturated maximum limit was not reached. The amount of mShh conjugated to the IPN at 1 μ*M* input concentration was equivalent to the amount of mShh nonspecifically adsorbed at 50 n*M* input concentration to TCPS (data not shown). Attendant to the stated equivalence is the assumption that the accessibility of the His tag to the HRP probe was not substantially different between these two scenarios. As such, *in vitro* experiments compared an input grafting concentration of 1 μ*M* mShh to the IPN surfaces against groups treated with 50 n*M* soluble mShh. In doing so, the functional amount of mShh either immobilized or adsorbed was assumed to be equivalent and allowed for direct comparisons of bioactivity between adsorbed mShh on TCPS surfaces and immobilized mShh on IPN surfaces.

The most significant result of our study was that the IPN/RGD/Shh surface supplemented with BMP-2/4 (IPN/RGD/Shh 24) had the highest growth rate and ALP activity among all groups at day 5, and resulted in significantly higher ALP normalized activity than IPN/RGD supplemented with soluble mShh and BMP-2/4 (IPN/RGD S24), its comparable soluble mShh analog, at all time points. At 3, 5, and 7 days, the values (in units of μU ALP/μg protein) were 13.5 ± 0.7 vs. 11.6 ± 0.8 ($p = 0.001$), 27.1 ± 1.6 vs. 20.9 ± 0.5 ($p < 0.001$), and 11.1 ± 0.3 vs. 7.2 ± 0.3 ($p < 0.001$), respectively, using the Tukey-Kramer HSD test of significance against all tested groups. Thus, the transforming effect of immobilized mShh was enhanced relative to soluble mShh for the BMSC culture model.

Regarding the activity of the peptide, bsp-RGD (15), the IPN/RGD surface without supplements was able to support elevated ALP activity compared with TCPS. Therefore, it appears that bsp-RGD (15) functions as a mild promoter of differentiation, which is consistent with our previous observations.[3,14,15] The IPN/RGD surfaces also had higher growth rates than TCPS surfaces in each media supplementation category (Table III). Therefore, in contrast to a previously published report which found that RGD coatings alone failed to support mesenchymal stem cell

proliferation and spreading,[40] the growth rate on bsp-RGD (15) was greater than on TCPS. The difference in observation may be attributed to either the method of peptide presentation or the peptide sequence itself. Regarding the latter, Harbers and Healy[15] showed that residues surrounding RGD as well as the overall conformation of the peptide significantly influenced the matrix mineralization behavior of osteoblast-like cells, and that short peptide sequences dominated by the RGD group have dramatically reduced activity.

In contrast to positive *in vitro* observations with bsp-RGD (15), we and others have shown that interfaces decorated with RGD-containing peptides do not improve peri-implant bone formation and interfacial bonding *in vivo*.[9,10,12] Interestingly, the magnitudes of the interfacial shear strength data at 4 weeks from these studies were similar in magnitude, $\sim$0.14–0.38 MPa, suggesting a common failure mode. The dichotomy between *in vitro* and *in vivo* observations could be due to the attenuation of the RGD signal by other stronger mitogens and morphogens contained within the fibrin clot initially surrounding the implant. As such, this study explored the potential use of Shh as a more powerful agent in directing cell behavior. Furthermore, although bsp-RGD (15) was intended to impart specificity to osteoblasts at the implant site it likely upregulated mitogenic responses in other cells present that exploit the $\alpha_v\beta_3$ integrin for cell adhesion. Thus, it is possible that other peptides targeting differential integrin specificity (e.g., the collagen receptor, $\alpha_2\beta_1$) may prove to be beneficial in influencing bone healing in the peri-implant region.[41,42]

We have demonstrated positive mitogenic and differentiating effects of immobilized mShh, in conjunction with soluble BMP-2 and BMP-4, on adult rat BMSCs. Differentiation of this uncommitted and heterogeneous cell population into the osteoblast phenotype was substantially enhanced with grafted mShh compared with mShh in soluble form. Moreover, we have described a straightforward method for quantifying the surface density of a His-tagged recombinant protein (e.g., mShh). Future work will explore whether the immobilized mShh/IPN-RGD surface can improve bone implant contact and bone formation in the rat femoral ablation model *in vivo*.

References

1. Massia SP, Hubbell JA. Covalently grafted RGD- and YIGSR-containing synthetic peptides support receptor-mediated adhesion of cultured fibroblasts. Anal Biochem 1990;187:292–301.
2. Drumheller PD, Hubbell JA. Polymer networks with grafted cell adhesive peptides for highly biospecific cell adhesive substrates. Anal Biochem 1994;222:380–388.
3. Rezania A, Healy KE. Biomimetic peptide surfaces that regulate adhesion, spreading, cytoskeletal organization, and mineralization of the matrix deposited by osteoblast-like cells. Biotechnol Prog. 1999;15:19–32.
4. Kisiday J, Jin M, Kurz B, Hung H, Semino C, Zhang S, Grodzinsky AJ. Self-assembling peptide hydrogel fosters chondrocyte extracellular matrix production and cell division: Implications for cartilage tissue repair. Proc Natl Acad Sci USA 2002;99:9996–10001.
5. Holmes TC, de Lacalle S, Su X, Liu G, Rich A, Zhang S. Extensive neurite outgrowth and active synapse formation on self-assembling peptide scaffolds. Proc Natl Acad Sci USA 2000;97:6728–6733.
6. Cavalcant-Adam EA, Shapiro IM, Composto RJ, Macarak EJ, Adams CS. RGD peptides immobilized on a mechanically deformable surface promote osteoblast differentiation. J Bone Miner Res 2002;17:2130–2140.
7. Kirkwood K, Rheude B, Kim YJ, White K, Dee KC. In vitro mineralization studies with substrate-immobilized bone morphogenetic protein peptides. J Oral Implantol 2003;29:57–65.
8. Schliephake H, Scharnweber D, Dard M, Rossler S, Sewing A, Meyer J, Hoogestraat D. Effect of RGD peptide coating of titanium implants on periimplant bone formation in the alveolar crest: An experimental pilot study in dogs. Clin Oral Implants Res 2002;13:312–319.
9. Elmengaard B, Bechtold JE, Soballe K. In vivo effects of RGD-coated titanium implants inserted in two bone-gap models. J Biomed Mater Res 2005;75A:249–255.
10. Ferris DM, Moodie GD, Dimond PM, Gioranni CWD, Ehrlich MG, Valentini RF. RGD-coated titanium implants stimulate increased bone formation in vivo. Biomaterials 1999;20:2323–2331.
11. Schliephake H, Scharnweber D, Dard M, Sewing A, Aref A, Roessler S. Functionalization of dental implant surfaces using adhesion molecules. J Biomed Mater Res B Appl Biomater 2005;73:88–96.
12. Barber TA, Ho JE, De Ranieri A, Virdi AS, Sumner DR, Healy KE. Peri-implant bone formation and implant integration strength of peptide-modified p(AAm-co-EG/AAc) IPN coated titanium implants. J Biomed Mater Res A 2007;80:306–320.
13. Barber TA, Gamble LJ, Castner DG, Healy KE. In vitro characterization of peptide-modified p(AAm-co-EG/AAc) IPN coated titanium implants. J Orthop Res 2006;24:1366–1376.
14. Rezania A, Healy KE. The effect of peptide surface density on the mineralization of matrix deposited by osteogenic cells. J Biomed Mater Res 2000;52:595–600.
15. Harbers GM, Healy KE. The effect of ligand type and density on osteoblast adhesion, proliferation, and matrix mineralization. J Biomed Mater Res 2005;75:855–869.
16. Kuhl PR, Griffith-Cima LG. Tethered epidermal growth factor as a paradigm for growth factor-induced stimulation from the solid phase. Nat Med 1996;2:1022–1027.
17. De Ranieri A, Virdi AS, Kuroda S, Shott S, Dai Y, Sumner DR. Local application of rhTGF-beta 2 modulates dynamic gene expression in a rat implant model. Bone 2005;36:931–940.
18. Ingham PW, McMahon AP. Hedgehog signaling in animal development: Paradigms and principles. Genes Dev 2001; 15:3059–3087.
19. Bitgood MJ, McMahon AP. Hedgehog and Bmp genes are coexpressed at many diverse sites of cell–cell interaction in the mouse embryo. Dev Biol 1995;172:126–138.
20. Roelink H. Tripartite signaling of pattern: Interactions between hedgehogs, BMPs and Wnts in the control of vertebrate development. Curr Opin Neurobiol 1996;6:33–40.
21. Spinella-Jaegle S, Rawadi G, Kawai S, Gallea S, Faucheu C, Mollat P, Courtois B, Bergaud B, Ramez V, Blanchet AM,

Adelmant G, Baron R, Roman-Roman S. Sonic hedgehog increases the commitment of pluripotent mesenchymal cells into the osteoblastic lineage and abolishes adipocytic differentiation. J Cell Sci 2001;114:2085–2094.
22. Yamaguchi A, Komori T, Suda T. Regulation of osteoblast differentiation mediated by bone morphogenetic proteins, hedgehogs, and Cbfa1. Endocr Rev 2000;21:393–411.
23. Zehentner BK, Leser U, Burtscher H. BMP-2 and Sonic hedgehog have contrary effects on adipocyte-like differentiation of C3H10T1/2 cells. DNA Cell Biol 2000;19:275–281.
24. Kawai S, Sugiura T. Characterization of human bone morphogenetic protein (BMP)-4 and -7 gene promoters: Activation of BMP promoters by Gli, a Sonic hedgehog mediator. Bone 2001;29:54–61.
25. Shea CM, Edgar CM, Einhorn TA, Gerstenfeld LC. BMP treatment of C3H10T1/2 mesenchymal stem cells induces both chondrogenesis and osteogenesis. J Cell Biochem 2003;90:1112–1127.
26. Edwards PC, Ruggiero S, Fantasia J, Burakoff R, Moorji SM, Paric E, Razzano P, Grande DA, Mason JM. Sonic hedgehog gene-enhanced tissue engineering for bone regeneration. Gene Ther 2005;12:75–86.
27. Kuroda S, Virdi AS, Dai Y, Shott S, Sumner DR. Patterns and localization of gene expression during intramembranous bone regeneration in the rat femoral marrow ablation model. Calcif Tissue Int 2005;77:212–225.
28. Yuasa T, Kataoka H, Kinto N, Iwamoto M, Enamoto-Iwamoto M, Iemura S-I, Ueno N, Shibata Y, Kurosawa H, Yamaguchi A. Sonic hedgehog is involved in osteoblast differentiation by cooperating with BMP-2. J Cell Physiol 2002;193:225–232.
29. Barber TA, Harbers GM, Park S, Gilbert M, Healy KE. Ligand density characterization of peptide-modified biomaterials. Biomaterials 2005;26:6897–6905.
30. Ho JE, Barber TA, Virdi AS, Sumner DR, Healy KE. The effect of enzymatically degradable IPN coatings on periimplant bone formation and implant fixation. J Biomed Mater Res A 2007;81A:720–727.
31. Kuroda S, Virdi AS, Li P, Healy KE, Sumner DR. A low-temperature biomimetic calcium phosphate surface enhances early implant fixation in a rat model. J Biomed Mater Res 2004;70:66–73.
32. Krishnan V, Ma YFL, Moseley JM, Geiser AG, Friant S, Frolik CA. Bone anabolic effects of Sonic/Indian hedgehog are mediated by BMP-2/4-dependent pathways in the neonatal rat metatarsal model. Endocrinology 2001;142:940–947.
33. Williams KP, Rayhorn P, Chi-Rosso G, Garber EA, Strauch KL, Horan GSB, Reilly JO, Baker DP, Taylor FR, Koteliansky V, Pepinsky RB. Functional antagonists of sonic hedgehog reveal importance of the N terminus for activity. J Cell Sci 1999;112:4405–4414.
34. Bearinger JP, Castner DG, Healy KE. Biomolecular modification of p(AAm-co-EG/AA) IPNs supports osteoblast adhesion and phenotypic expression. J Biomater Sci Polym Ed 1998;9:629–652.
35. Harbers GM, Gamble LJ, Irwin EF, Castner DG, Healy KE. Development and characterization of a high-throughput system for assessing cell-surface receptor-ligand engagement. Langmuir 2005;21:8374–8384.
36. Nieba L, Nieba-Axmann SE, Persson A, Hamalainen M, Edebratt F, Hansson A, Lidholm J, Magnusson K, Karlsson A, Pluckthun A. BIACORE analysis of histidine-tagged proteins using a chelating NTA sensor chip. Anal Biochem 1997; 252:217–228.
37. Thieme HR. Classic Models of Density-Dependent Population Growth for Single Species. Mathematics in Population Biology. Princeton: Princeton University Press; 2003.
38. De Ranieri A, Virdi AS, Kuroda S, Healy KE, Hallab NJ, Sumner DR. Saline irrigation does not affect bone formation or fixation strength of hydroxyapatite/tricalcium phosphate-coated implants in a rat model. J Biomed Mater Res B Appl Biomater 2005;74:712–717.
39. Hall TMT, Porter JA, Beachy PA, Leahy DJ. A potential catalytic site revealed by the 1.7-Å crystal structure of the amino-terminal signalling domain of Sonic hedgehog. Nature 1995; 378:212–216.
40. Sawyer AA, Hennessy KM, Bellis SL. Regulation of mesenchymal stem cell attachment and spreading on hydroxyapatite by RGD peptides and adsorbed serum proteins. Biomaterials 2005;26:1467–1475.
41. Reyes CD, Garcia AJ. Engineering integrin-specific surfaces with triple-helical collagen-mimetic peptide. J Biomed Mater Res A 2003;65:511–523.
42. Reyes CD, Garcia AJ. Alpha2beta1 integrin-specific collagen-mimetic surfaces supporting osteoblastic differentiation. J Biomed Mater Res A 2004;69:591–600.